



Electrostatic complexation of linear polyelectrolytes with soft spherical nanoparticles



Qianqian Cao ^{*}, Michael Bachmann ^{*}

Center for Simulational Physics, The University of Georgia, Athens, GA 30602, USA

ARTICLE INFO

Article history:

Received 12 July 2013

In final form 4 September 2013

Available online 11 September 2013

ABSTRACT

We use Langevin molecular dynamics simulations to study the complexation of a linear polyelectrolyte (LPE) chain with an oppositely charged soft nanoparticle, modeled by a spherical polyelectrolyte brush (SPB). By changing core radius of the SPB and length of polyelectrolyte (GPE) chains grafted at it, a structural transition from a charged, LPE-covered sphere via a softer nanobrush toward a star-like polyelectrolyte is identified. As a result, the LPE chain develops various wrapping conformations around the SPB. Our systematic analysis reveals all relevant conformational binding modes for the polyelectrolyte–nanoparticle complex.

© 2013 Elsevier B.V. All rights reserved.

1. Introduction

Unraveling the variety and understanding the stability of structures of macromolecules in complexes formed with soft and solid nano-objects is decisive for the appreciation of their relevance in biological systems (such as DNA–histone complexes) and their potential for nano- and biotechnological applications (e.g., as nano-transporters and biosensors) [1,2]. The complexity of a systematic investigation unveils itself in its entirety, if one takes into account that this kind of complexation is a non-local, but not macroscopic, cooperative process on mesoscopic scales. Meso-molecular physics is little understood, because finite-size effects are integral for structure formation on this length scale, but can hardly be studied theoretically, let alone experimentally. Because cooperativity is essential, mesoscopic structure formation processes resemble phase transitions in macroscopic systems and, therefore, must have generic signatures, i.e., coarse-grained investigations will allow to capture the most significant features of the physisorption process that we will discuss in the following. The only available tool to extend our knowledge is the computer simulation of such systems. A systematic approach, such as the one described here, yields structural phase diagrams in parameter space that help identify those scenarios that are most relevant for biological adsorption processes and most interesting for technological applications.

In this Letter, we systematically study the complexation of a linear polyelectrolyte (LPE) with a soft nanoparticle. The nanoparticle is modeled as a spherical polyelectrolyte brush (SPB) consisting of a solid, impenetrable core and a surface layer of grafted

polyelectrolytes (GPEs) [3,4]. This is particularly interesting, because not only the LPE experiences structural transitions upon binding, but also the overall shape of the nanoparticle depends on its size and the properties of the GPE layer (grafting density and GPE length). The shape can even change in the complexation process. Various computational and analytical studies on the complexation of linear polyelectrolytes (LPE) with oppositely charged nanoparticles have already been performed [5–16]. These investigations have addressed properties of polyelectrolyte–nanoparticle complexes and effects of different environments (including temperature, salt concentration, surface charge density and size of the particle, chain length, linear charge density and stiffness of the polyelectrolyte) on the conformational behavior of adsorbed polyelectrolytes. It turned out that adsorption affinity and equilibrium structure of the polyelectrolyte on the particle surface sensitively depend on the competition between chain intrinsic stiffness, electrostatic repulsion among charged monomers, and electrostatic attractive interaction between the monomers and the particle.

Polyelectrolytes adsorbed on oppositely charged bare and *impenetrable* solid surfaces can be regarded as well-understood systems. However, insufficient attention has been paid to understand the complexation of polyelectrolytes with penetrable objects (such as branched polymers) at molecular level by theoretical modeling and simulations [17–21,4], although numerous experiments have reported such complexation to occur [22–24]. These are very interesting systems, because the dendrimers can act as nanocontainers to control the drug delivery and release processes. If the “guest” molecules are LPE chains, typically DNA, the formed complexes are promising candidates for potential biomedical applications [24]. Soft nanoparticles do not possess a clearly defined surface and allow polyelectrolytes to penetrate inside, which leads to a more complicated local structure. Understanding the

^{*} Corresponding authors.

E-mail addresses: qqcao@uga.edu (Q. Cao), bachmann@smsyslab.org (M. Bachmann).

formation mechanism of the complexes of penetrable objects with polyelectrolytes and the effects of chain structures (such as chain stiffness, arm number and topology of branched polymers) on the conformational behavior of the complexes is essential to construct and design complexes with specific function and morphology. Recent investigations indicated that as the stiffness of LPE chain increases, it undergoes different conformational transitions [20,21]. Moreover, the dependence of the size and the shape of charged dendrimer on the LPE stiffness and Bjerrum length was investigated [20].

Here, we study the complexation of an LPE chain and a spherical polyelectrolyte brush (SPB) with a penetrable grafted polyelectrolyte (GPE) layer [3], using coarse-grained molecular dynamics simulations. It is expected that increasing the length of the GPEs will change the surface properties of the SPB from bare and impenetrable to soft and penetrable, before it forms a star-like polyelectrolyte. This would cause a potentially interesting conformational behavior of the polyelectrolyte–SPB complex, which will be in our focus here. Compared to the branched polymers, the conformation of the complexed LPE with the SPB does not only depend on the structure of the penetrable brush layer but also on the confinement of the core surface.

2. Simulation method and model

Coarse-grained MD has been adopted to improve computational efficiency by neglecting the local atomistic details. From a solvent model viewpoint, coarse-grained models can be divided into implicit and explicit solvent models. In the implicit solvent model used in this Letter, solvent effects are effectively modeled by the non-bonded interaction. Especially in dilute polymer solutions, tracking the dynamics of solvent molecules is time-consuming and generally not of interest. Recently, such models were used for studying the interaction between dendrimer and LPE [20,17], the formation of micelles [25], and the complexation between charged surfactants and SPB [26].

The SPB considered in this Letter consists of a spherical core uniformly grafted with N_g fully flexible GPE chains. Each of these possesses N_{gm} positively charged monomers. The LPE chain contains $N_{lm} = 200$ negatively charged monomers. $N_{ci} = N_g N_{gm} + N_{lm}$ monovalent ions are included in the system, where $N_{gm} N_g$ anions and N_{lm} cations are dissociated from the GPE and LPE chains, respectively. We limit the total amount of charges on the SPB to a fixed value, $N_{gm} N_g = 300$. All particles are enclosed in a cubic simulation box with edge lengths $L = 250\sigma$, where σ is the particle diameter. We chose it to be the same for all particle types. Periodic boundary conditions are applied in all three directions. Our simulation box is large enough to avoid short-range interactions of the LPE chain with its periodic images. The purely repulsive short-range interaction between any two particles separated by a distance r is modeled by the truncated-shifted Lennard-Jones (LJ) potential with the interaction strength ϵ_{LJ} and the particle diameter σ . Adjacent monomers in the GPE and LPE chains are coupled by a finitely extensible nonlinear elastic (FENE) potential with the maximum bond length $R_0 = 1.5\sigma$ and the spring constant $k_l = 30\epsilon_{LJ}/\sigma^2$ [27]. One end monomer of each GPE chain is anchored at the surface of the SPB. All particles except the grafted monomers interact repulsively with the core through a LJ potential with a shifted distance of the core radius R . The bending rigidity of the LPE chain is modeled using a harmonic angle potential with the stiffness $k_\theta = 300\epsilon_{LJ}/rad^2$. Electrostatic interaction between any two charged particles is described by the Coulomb potential. We set the Bjerrum length $\lambda_B = e^2/(4\pi\epsilon_0\epsilon_r k_B T)$ to σ , which is about 0.7 nm for water at room temperature. ϵ_0 is the vacuum permittivity and the dielectric constant of the solvent is $\epsilon_r = 80.4$. The sum

of long-range electrostatic interactions is calculated using the particle-particle/particle-mesh (PPPM) algorithm [28]. For a more detailed description of our model, see Ref. [4].

The system temperature is controlled by a Langevin thermostat [29]. We set the friction coefficient $\gamma = 1.0\tau^{-1}$ with the time unit $\tau = (m\sigma^2/\epsilon_{LJ})^{1/2}$ and the system temperature $T = \epsilon_{LJ}/k_B$ which represents room temperature. Our simulations are conducted with a time step $\Delta t = 0.008\tau$. Initially, the counterions are randomly dispersed within the simulation region. An equilibrium run of 1×10^6 time steps was performed first, then followed by a production run of 2×10^6 time steps to obtain the equilibrium properties of the system. We utilize the Large-scale Atomic/Molecular Massively Parallel Simulator (LAMMPS) [30] to perform classical molecular dynamics simulations.

3. Results and discussions

One of our major results is that an increase of the GPE length promotes a substantial change of the surface structure of the SPB, which can behave like a charged bare sphere, a polyelectrolyte brush, or a star-like polyelectrolyte. If the nanoparticle has a brush-like structure, both, the core surface and the characteristics of grafted layer, will become important in determining the conformational behavior of the LPE. Figure 1 illustrates a series of typical morphologies of the LPE–SPB complex in thermodynamic equilibrium at temperature T found in our simulations for various core radii and GPE lengths [4]. In the extreme case $N_{gm} = 1$, the LPE chain directly adsorbs to the core surface and adopts an ordered spool-like structure, which is similar to single nucleosomes [31]. Upon increasing the chain length, it detaches from the core surface. In the cases of long GPE chains ($N_{gm} = 20$ and 50) and large core radius ($R = 21\sigma$), a more favorable “S”-shape conformation is formed. When the core radius is reduced significantly, to minimize conformational free energy the long GPE chains are stretched and located in a plane together with the LPE chain which does not exhibit a well-defined solenoid conformation but rather forms a knot near the core. Clearly, some GPE chains of $N_{gm} = 50$ are deflected by the LPE chain at $R = 7\sigma$ and 10σ . The deflected part of grafted chains (namely the chain segment complexed to the LPE) is still in an extended state, and the non-adsorbed segment is also straightened. Note that the end segments of the LPE are not bent by the drag force from long grafted chains. In contrast, the end segments of grafted chains which are entangled on the ends of the LPE chain, adopt the extended conformation of end segments of the LPE chain.

Figure 2a shows the radius of gyration of the LPE chain $\langle R_{lg} \rangle$ as a function of N_{gm} for different core radii. The LPE chain swells as the GPE length increases, especially for small core radii. The GPE length has a weak effect on $\langle R_{lg} \rangle$ when the core radius becomes larger. For $N_{gm} < 30$, no significant change is observed at $R = 30\sigma$. This means that the core radius starts dominating control of the conformational behavior of the LPE. Only if the LPE chain becomes longer compared to the diameter of the core, the LPE chain starts swelling. For very small core radius and long GPE chains, the surface confinement of the core no longer influences the LPE conformation. The LPE chain tends to cross near the core.

For a quantitative study of the complexation degree between the LPE and grafted chains, we calculate the ratio $\chi = \langle N_{ads} \rangle / N_{lm}$, where $\langle N_{ads} \rangle$ denotes the canonical average number of GPE monomers which are in contact with the LPE. $\langle N_{ads} \rangle$ can be obtained by counting all monomers of grafted chains within a sphere centered at the center of mass of each LPE monomer and with the cutoff radius $r_c = 1.5\sigma$. Each monomer of the grafted chain is counted only once. The result in Figure 2b indicates that high surface charge density for small cores strongly confines the LPE to the core

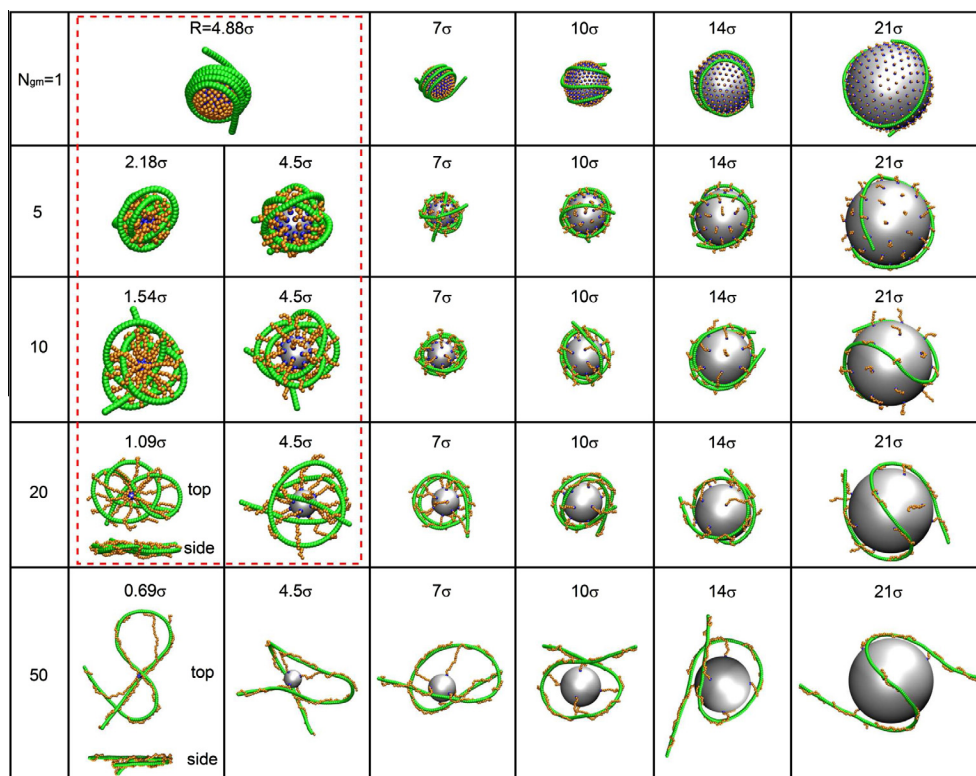


Figure 1. Typical simulation snapshots of LPE-SPB complexes for fixed number of surface charges, $N_g N_{gm} = 300$, at temperature T . The first row ($N_{gm} = 1$) shows the conformations of the semiflexible LPE which wraps around the core. Upon increasing the GPE length, the bending energy of the LPE chain is released to a certain extent and the LPE is confined in more extended structures. The LPE and GPE chains are shown in green and orange, respectively. Blue and gray beads represent grafted monomers and spherical core, respectively. For clarity, the snapshots surrounded by the red frame are enlarged and not to scale. (For interpretation of the references to colour in this figure legend, the reader is referred to the web version of this article.)

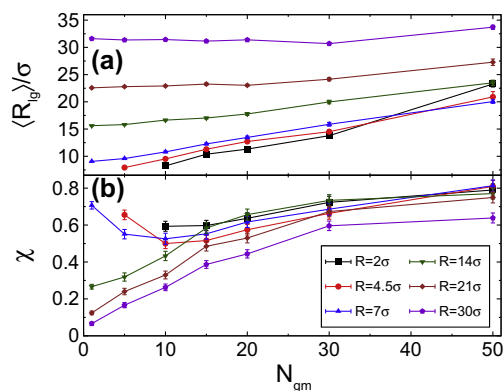


Figure 2. (a) Average radius of gyration of the LPE ($\langle R_{lg} \rangle$) and (b) complexation degree χ of the LPE with the GPE chains as a function of the GPE length for different values of the core radius R .

surface, and thus more contacts between the LPE and GPE monomers are favored. Additionally, to condense the LPE chain to a compact state, more GPE monomers are necessary. Complexation to the LPE chain requires stronger pulling force. We find that long grafted chains are more supportive of complexation. At $R = 30\sigma$, because of a wide separation between the grafting points, the probability for forming contacts between the LPE and GPE chains is largely reduced. For short GPE chains, the increase of the core radius significantly suppresses the complexation. This indicates that the core radius becomes large enough that the LPE chain bound to neighboring grafted chains is out of reach for some GPE chains.

Effectively, the binding between LPE and GPEs is weaker, if the complexation degree is not too high. This is advantageous in

applications or for biosystems, where LPE cargo has to be released at the destination. As we see in Figure 2b, for small cores ($R = 2\sigma, 4.5\sigma, 7\sigma$), the complexation degree χ depends on the length of the GPE chains and even exhibits a minimum (near $N_{gm} = 10$). In this case, many of the GPE chains ($N_g = 30$ for $N_{gm} = 10$) can not bind to the semiflexible LPE, because they are too short and the grafting density is too small. Thus, for the design of a synthetic soft nanoparticle, it is important to take into account the effects of GPE length and density upon LPE binding.

To gain a further understanding of the effect of the core radius on the LPE structure, we plot the density distribution function $P(r)$ of the LPE monomers along the radial direction of the core for different core radii in Figure 3. The peak of $P(r)$ increases with the

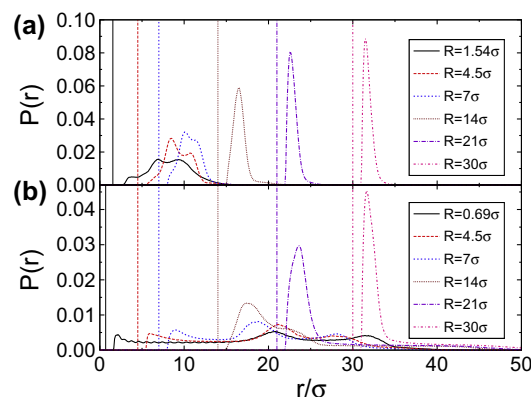


Figure 3. Distribution function $P(r)$ of the LPE monomers with the chain length (a) $N_{gm} = 10$ and (b) 50 along the radial direction of the core. The vertical lines represent the position of the core surface.

core radius. When $R \leq 7\sigma$, several peaks are developed. A larger separation between the peaks at $N_{gm} = 50$ is observed due to the swollen conformation of the LPE chain (Figure 3b). Note that the distribution profile contracts as the core radius increases ($R \leq 7\sigma$), but its outside (right in this figure) border does not shift significantly. Thus, the peripheral size of the LPE chain is less influenced in this range of core radius. The secondary peaks disappear as the core radius further increases. At $R = 30\sigma$, the peak becomes very pronounced and its location is closer to the core surface, which indicates most LPE segments distribute near the surface.

Obviously, at small values of R the high bending energy due to strong shrinkage of the LPE chain forces grafted chains to stretch. This is evident from Figure 4, where we plot the shape factor $\langle R_{eg}^2/R_{gg}^2 \rangle$ of the GPE chains as a function of R for different GPE lengths. R_{eg} and R_{gg} denote the end-to-end distance and radius of gyration of the GPE chains, respectively. For small values of R , a reduction in the shape factor upon increasing the core radius is caused by the release of bending energy of the LPE, which corresponds to an increase of $\langle R_{lg} \rangle$, until a minimum value is reached. A further increase of the core radius results in a growing shape factor because the radius of gyration of the LPE chain becomes larger (Figure 2a). Moreover, the local LPE segments also significantly stretch out, especially for large core radii. The local extension brings about stretched conformations of the GPE chains complexed to the LPE chain. For short GPE chains with $N_{gm} = 5$ (Figure 2b), the complexation degree sharply drops with increasing core radius. Thus, the asymptotic value of $\langle R_{eg}^2/R_{gg}^2 \rangle$ represents approximately the shape factor of free GPE chains. The decrease of the shape factor for $N_{gm} = 50$ at large core radius $R = 30\sigma$ is a finite-size effect due to the very low density of GPEs.

In complexation processes of polyelectrolytes and oppositely charged objects the counterions are released into the solution [32], due to stronger electrostatic correlation between them. Here, to characterize the counterion release we present the densities of different components along the radial direction of the core in Figure 5. It is clear that the counterions are almost depleted near the core for the nanoparticle-like case $N_{gm} = 1$. Only a slight amount of GPE counterions is adsorbed on the core for a moderate compensation of electrostatic attraction from non-screened surface charges. For the longer GPE chains of $N_{gm} = 20$, the density of the LPE monomers is consistent with that of the GPE monomers in the region away from the core surface, which indicates a complete GPE and LPE complexation. However, there is a higher density of GPE counterions near the core. For $N_{gm} = 20$ and $R = 7\sigma$, in which case the GPE length is comparable with the core diameter, the LPE chain does not reside close to the surface of the core (see Figure 1). The considerable chain rigidity of the LPE leads to a swelling conformation [4]. GPE counterions adsorb at the core to neutralize GPE

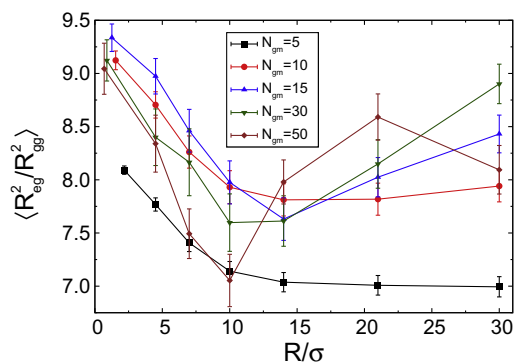


Figure 4. Shape factor $\langle R_{eg}^2/R_{gg}^2 \rangle$ of the GPE chains as a function of the core radius for different values of the GPE length N_{gm} .

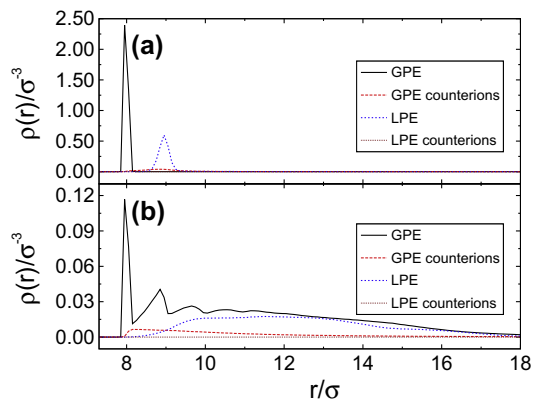


Figure 5. Densities of the LPE and GPE monomers as well as corresponding counterions along the radial direction of the core with $R = 7\sigma$ at (a) $N_{gm} = 1$ and (b) 20.

monomers near the core surface. Similarly to the case of $N_{gm} = 1$, the LPE counterions are fully depleted from the complex.

4. Conclusions

To summarize, our simulations enabled a first systematic analysis of the complexation of a LPE chain with an SPB for a wide range of core radii and GPE lengths. The results show that, compared to the complexation of the LPE chain with a bare charged sphere, the LPE chain exhibits more complex and diverse conformations when it is complexed to an SPB, which mimics a soft nanoparticle. The increase of the GPE length leads to a release of the bending energy of the LPE chain and favors complexation. The conformational behavior of the LPE chain depends entirely on the structural parameters of the SPB. From the energetic perspective, the morphology of the LPE–SPB complex is dominated by the electrostatic attraction between the LPE and SPB chains which favors complexation, and the extension of the LPE chain induced by the repulsive monomer–monomer interaction and intrinsic rigidity which restricts complexation. The conformational degrees of freedom of the long GPE chains significantly contribute to the conformational transitions the LPE experiences upon complex formation. Additionally, the confinement of LPE conformations at the core surface depends on the ratio of the size of the core and the GPE length. The shape of the complex of biomacromolecules with soft nanoparticles plays a critical role in emerging nanomedicines with potential applications such as drug delivery and membrane permeability. The SPBs as a kind of nanoscaled materials with soft surface and solid core possess well-defined structures including controllable core size and physicochemical properties of the surface layer. The present Letter suggests further investigations such as at variable LPE stiffness and solution environment (especially salt valence and concentration) to obtain a systematic understanding of the LPE–SPB complexes.

Acknowledgement

This Letter is partially supported by the NSF Grant DMR-1207437 and by CNPq Grant 402091/2012-4.

References

- [1] A.V. Dobrynin, M. Rubinstein, *Prog. Polym. Sci.* 30 (2005) 1049.
- [2] R.R. Netz, D. Andelman, *Phys. Rep.* 380 (2003) 1.
- [3] M. Ballauff, *Prog. Polym. Sci.* 32 (2007) 1135.
- [4] Q. Cao, M. Bachmann, *Soft Matter* 9 (2013) 5087.
- [5] E.M. Mateescu, C. Jeppesen, P. Pincus, *Europhys. Lett.* 46 (1999) 493.
- [6] S.Y. Park, R.F. Bruinsma, W.M. Gelbart, *Europhys. Lett.* 46 (1999) 454.
- [7] P. Chodanowski, S. Stoll, *Macromolecules* 34 (2001) 2320.

- [8] P. Chodanowski, S. Stoll, *J. Chem. Phys.* 115 (2001) 4951.
- [9] S. Stoll, P. Chodanowski, *Macromolecules* 35 (2002) 9556.
- [10] S. Ulrich, A. Laguerre, S. Stoll, *Macromolecules* 38 (2005) 8939.
- [11] R. Messina, C. Holm, K. Kremer, *J. Chem. Phys.* 117 (2002) 2947.
- [12] A. Akinchina, P. Linse, *Macromolecules* 35 (2002) 5183.
- [13] A. Akinchina, P. Linse, *J. Phys. Chem. B* 107 (2003) 8011.
- [14] R.G. Winkler, A.G. Cherstvy, *Phys. Rev. Lett.* 96 (2006) 066103.
- [15] A. Chremos, A.Z. Panagiotopoulos, *Phys. Rev. Lett.* 107 (2011) 105503.
- [16] B.M. Rubenstein, I. Coluzza, M.A. Miller, *Phys. Rev. Lett.* 108 (2012) 208104.
- [17] S.V. Lyulin, A.A. Darinskii, A.V. Lyulin, *Macromolecules* 38 (2005) 3990.
- [18] P.K. Maiti, B. Bagchi, *Nano Lett.* 6 (2006) 2478.
- [19] S. Lyulin, K. Karatasos, A. Darinskii, S. Larin, A. Lyulin, *Soft Matter* 4 (2008) 453.
- [20] W.-d. Tian, Y.-q. Ma, *Macromolecules* 43 (2010) 1575.
- [21] J.S. Kos, J.U. Sommer, *Macromol. Theory Simul.* 21 (2012) 448.
- [22] E.R. Gillies, J.M. Fréchet, *Drug Discov. Today* 10 (2005) 35.
- [23] J.B. Wolinsky, M.W. Grinstaff, *Adv. Drug Delivery Rev.* 60 (2008) 1037.
- [24] C. Dufès, I.F. Uchegbu, A.G. Schätzlein, *Adv. Drug Delivery Rev.* 57 (2005) 2177.
- [25] H. Noguchi, *Soft Matter* 8 (2012) 8926.
- [26] Q. Cao, C. Zuo, L. Li, *PCCP* 13 (2011) 9706.
- [27] K. Kremer, G.S. Grest, *J. Chem. Phys.* 92 (1990) 5057.
- [28] R.W. Hockney, J.W. Eastwood, *Computer Simulation Using Particles*, Adam Hilger, Bristol, 1988.
- [29] G.S. Grest, K. Kremer, *Phys. Rev. A* 33 (1986) 3628.
- [30] S. Plimpton, *J. Comp. Phys.* 117 (1995) 1.
- [31] T. Sakaue, K. Yoshikawa, S.H. Yoshimura, K. Takeyasu, *Phys. Rev. Lett.* 87 (2001) 078105.
- [32] F. Carnal, S. Stoll, *J. Phys. Chem. B* 115 (2011) 12007.